# Emergent Haldane phase in an alternating-bond $\mathbb{Z}_3$ parafermion chain

Shun-Yao Zhang,[1] Hong-Ze Xu,[1] Yue-Xin Huang,[1] Guang-Can Guo,[1,2] Zheng-Wei Zhou,[1,2,*] and Ming Gong[1,2,†]

[1]*CAS Key Laboratory of Quantum Information, University of Science and Technology of China, Hefei 230026, People's Republic of China*
[2]*Synergetic Innovation Center of Quantum Information and Quantum Physics, University of Science and Technology of China, Hefei, Anhui 230026, China*

The Haldane phase represents one of the most important symmetry-protected states in modern physics. This state can be realized using spin-1 and spin-$\frac{1}{2}$ Heisenberg models and bosonic particles. Here we explore the emergent Haldane phase in an alternating bond $\mathbb{Z}_3$ parafermion chain, which is different from the previous proposals from fundamental statistics and symmetries. We show that this emergent phase can also be characterized by a modified long-range string order, as well as fourfold degeneracy in the ground-state energies and entanglement spectra. This phase is protected by both the charge conjugate and parity symmetry, and the edge modes are shown to satisfy parafermionic statistics in which braiding of the two edge modes yields a $\frac{2\pi}{3}$ phase. This model also supports rich phases, including a topological ferromagnetic parafermion (FP) phase, trivial paramagnetic parafermion phase, classical dimer phase, and gapless phase. The boundaries of the FP phase are shown to be gapless and critical with central charge $c = 4/5$. Even in the topological FP phase, it is also characterized by long-range string order; thus we observe a drop of string order across the phase boundary between the FP phase and the Haldane phase. This work opens a new way for finding of exotic topological phases with parafermions.

Topological phases and associated phase transitions beyond the Landau paradigm of phase transition have been a major topic in modern physics [1–3]. Examples include topological insulators [4] and the Haldane phase [5,6]. In the noninteracting models in topological insulators and topological superconductors, these phases are characterized by integer numbers associated with time-reversal symmetry, particle-hole symmetry, and chiral symmetry [7,8]. However, in the strong interacting models such as Haldane phases, they are characterized by long-range string order and ground-state degeneracy. These phases can be used to realize exotic excitations with Abelian or non-Abelian statistics, which are building blocks for topological quantum computation. Along this line, the self-Hermitian Majorana zero modes [9] have been realized in experiments by several groups [10–15]. Moreover, the symmetry-protected Haldane phase has been proposed to be realized in spin-1 and spin-$\frac{1}{2}$ Heisenberg models [5,6,16,17], strong interacting bosonic models [18–23], and even fermionic models [24–27].

Here we are interested in the realization of the Haldane phase using $\mathbb{Z}_3$ parafermions [28–35], which is totally different from the above-mentioned models with regard to their fundamental statistics and symmetries. We consider an alternating-bond $\mathbb{Z}_3$ parafermion model, which can be realized in superconductor and $\nu = \frac{2}{3}$ fractional quantum Hall (FQH) hybrid structures [33,36]. This Haldane phase is characterized by nonlocal string order and fourfold degeneracy in both ground-state energies and entanglement spectra.

We map out the whole phase diagram and find some other exotic phases, including the ferromagnetic parafermion (FP) phase, paramagnetic parafermion (PP) phase, dimer phase, and critical gapless phase. The boundaries for the FP phase are critical with central charge $c = \frac{4}{5}$. The edge modes in the Haldane phase exhibit fractional Abelian braiding protected by charge conjugate symmetry and parity symmetry. This kind of emergent phenomena are rather general in parafermion models, and thus this work opens a new avenue in search of exotic symmetry-protected topological phases in parafermion models.

## I. MODEL

We consider the following alternating-bond $\mathbb{Z}_3$ parafermion chain ($\omega^3 = 1$):

$$H = -\omega^2 \left( \sum_{j=1}^{L} J_j(\delta)\, \alpha_{2j}^\dagger \alpha_{2j+1} + h\, \alpha_{2j-1}^\dagger \alpha_{2j} \right) + \text{H.c.}, \quad (1)$$

where $J_j(\delta) = 1 + (-1)^j\, \delta$, and $\alpha_j$ are parafermions satisfying $\alpha_j^3 = 1$, $\alpha_j^\dagger = \alpha_j^2$, and $\alpha_i \alpha_j = \alpha_j \alpha_i \omega^{\text{sgn}(j-i)}$. This model can be realized using the setup in Fig. 1(a) in the superconductor and FQH hybrid structure [39], in which the alternating bonds are controlled by the distance between the superconducting islands. This model is related to the following $\mathbb{Z}_3$ clock model via the Jordan-Wigner transformation: $\alpha_{2j-1} = \prod_{k \leqslant j-1} \tau_k \sigma_j$ and $\alpha_{2j} = \omega \sigma_j \prod_{k \leqslant j} \tau_k$, which yields [33,36]

$$H = -\sum_{i=1}^{L} [1 + (-1)^j \delta] \sigma_i^\dagger \sigma_{i+1} - h \sum_i \tau_i + \text{H.c.} \quad (2)$$
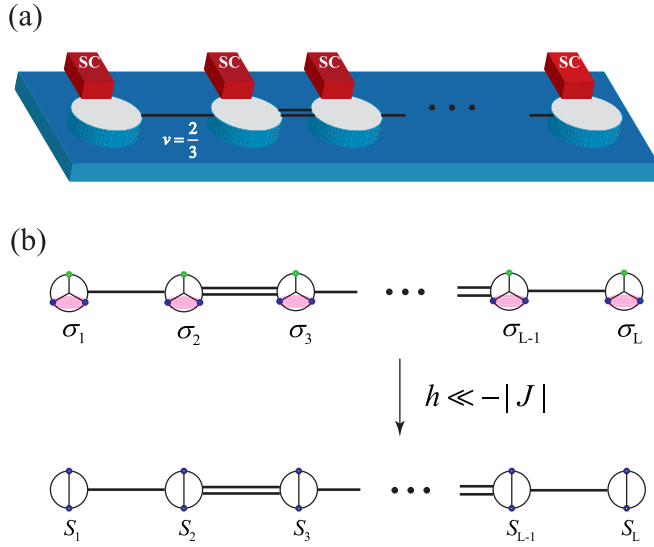
(a)



(b)

FIG. 1. (a) Realization of Eq. (1) using superconductor and $\nu = \frac{2}{3}$ FQH hybrid structure. The distance between the superconducting islands controls the coupling strengths between the parafermions localized at the holes, giving rise to the alternating-bond model. Other ideas for realizing of this model can be found in Refs. [31,33,37,38]. (b) Projection of the alternating-bond $\mathbb{Z}_3$ model to the spin-$\frac{1}{2}$ spin model in strong Zeeman field limit with $h \ll -J$.

We see that the second term plays the similar role as the magnetic field in $\mathbb{Z}_2$ spin models; thus $h$, for convenience, is termed as a Zeeman field. In the above, the operators satisfy $\sigma_i^3 = \tau_i^3 = 1$, $\sigma_i \tau_i = \omega \tau_i \sigma_i$, $\sigma_i^\dagger = \sigma_i^2$, and $\tau_i^\dagger = \tau_i^2$; all operators commute between different sites [28].

The $\mathbb{Z}_2$ symmetry is absent in the parafermion model. However, it can be restored by a projection from the $\mathbb{Z}_3$ to $\mathbb{Z}_2$ model [see Fig. 1(b)] when the highest state in each site is unoccupied. In the $h \gg -1$ limit, we obtain an equivalent $\mathbb{Z}_2$ spin model to the leading term as

$$H = -\sum_i [1 + (-1)^j \delta] s_i^\dagger s_{i+1} + \mathcal{O}(1/h^2), \quad (3)$$

where $s_i = s_i^x - i s_i^y$, with $s_i^\alpha$ being Pauli matrices. This staggered XX model has similar features as the staggered Heisenberg model discussed in literature [16,40,41] (see details in Ref. [42]), which support the Haldane phase when $\delta > 0$ and the trivial dimer phase when $\delta < 0$. We will show that this topological phase can be realized with even a modest Zeeman field $h$. This limiting case enables us to understand how the Haldane phase and related symmetries can emerge from the $\mathbb{Z}_3$ or even $\mathbb{Z}_k$ parafermions.

## II. PHASE DIAGRAM

We employ the density-matrix renormalization group (DMRG) method implemented by the ITENSOR project [43] and the exact diagonalization (ED) method to understand the phase diagram in Fig. 2. First, we look at $\delta = 0$, which supports several different critical points. The point at $h = J$ is self-dual [28,44] via $\mu_j = \prod_{k \leqslant j} \tau_k$ and $\nu_j = \sigma_j^\dagger \sigma_{j+1}$, which separates the threefold degenerate FP phase from the PP phase. This boundary was studied in literature [28,37]. When
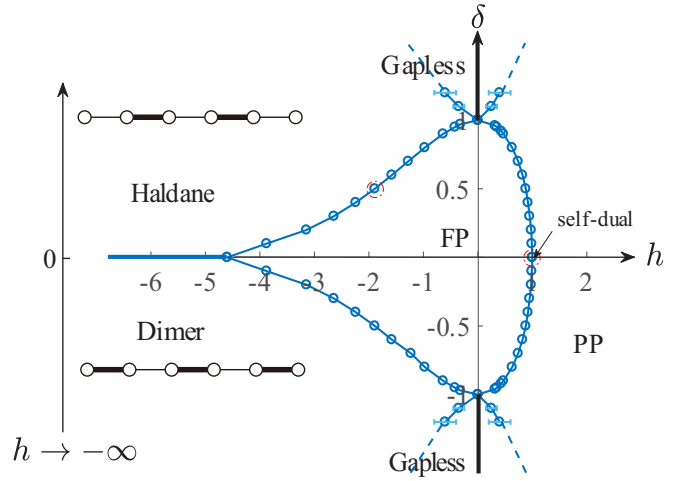


FIG. 2. Phase diagram of the alternating-bond parafermion model. FP and PP represent ferromagnetic and paramagnetic parafermion phase. The gapless phase with $|\delta| > 1$, $h \neq 0$ is critical with central charge $c = 1$.

$h < 0$, we find another critical point at $h_c = -4.6$. When $h < h_c$, the model is equivalent to the free fermion model or XX spin model, which is critical with central charge $c = 1$ [39,45–48]. This point was unveiled in Ref. [42]. On the other hand, when $h = 0$, this model is reduced to the classical Potts model, in which the $\sigma$ operators can be replaced by complex numbers $e^{ip2\pi/3}$ ($p = 0, 1, 2$) with critical points at $\delta = \pm 1$. At these two points, the chain is divided into short segments with length $\mathscr{L} = 4$, giving rise to an infinite-fold degenerate model. Similar infinite-fold degeneracy can be found when $|\delta| > 1$ for eigenvectors $|m_1 m_1 m_2 m_2 m_3 m_3 \cdots\rangle$, with $m_i \neq m_{i+1}$, where $m_i \in \{\uparrow, \searrow, \swarrow\}$ and $\{|\uparrow\rangle, |\searrow\rangle, |\swarrow\rangle\}$ are the eigenvectors of operator $\sigma$. This picture is similar to that in the extended parafermion model [42].

The line with $\delta = \pm 1$ can be solved exactly. We first focus on $\delta = +1$. In this case the model is decoupled into the following segments:

$$[\alpha_1 \alpha_2][\alpha_3 \alpha_4 \alpha_5 \alpha_6][\alpha_7 \alpha_8 \alpha_9 \alpha_{10}] \cdots [\alpha_{2L-1} \alpha_{2L}],$$

where the two parafermions block $[\alpha_1 \alpha_2]$ represent $h\omega^2 \alpha_1^\dagger \alpha_2 + \text{H.c.}$ and four parafermions block $[\alpha_i \alpha_j \alpha_k \alpha_l]$ represent $-h\omega^2 \alpha_i^\dagger \alpha_j - h\omega^2 \alpha_k^\dagger \alpha_l - 2J\omega^2 \alpha_j^\dagger \alpha_k + \text{H.c.}$ We can prove each block commutes with each other. The two edge modes are fully decoupled from all the other sites. When $h > 0$, the ground state of $h\omega^2 \alpha_1^\dagger \alpha_2 + \text{H.c.} = -h(\tau + \tau^\dagger)$ is unique, corresponding to the PP phase. In contrast, when $h < 0$, the ground states are twofold degenerate. For this reason, it corresponds to the Haldane phase with fourfold degeneracy, taking into account both ends. This picture is modified for the case with $\delta = -1$, which is decoupled into segments

$$[\alpha_1 \alpha_2 \alpha_3 \alpha_4][\alpha_5 \alpha_6 \alpha_7 \alpha_8] \cdots [\alpha_{2L-3} \alpha_{2L-2} \alpha_{2L-1} \alpha_{2L}].$$

We need only determine the properties of $H_4 = -h\omega^2 \alpha_1^\dagger \alpha_2 - h\omega^2 \alpha_3^\dagger \alpha_4 - 2J\omega^2 \alpha_2^\dagger \alpha_3 + \text{H.c.}$ When $h \gg J$ the ground state is $|0\rangle^{\otimes L}$. For $h \ll -|J|$, it is $\prod_i [|(2i)_2 (2i+1)_1\rangle + |(2i)_1 (2i+1)_2\rangle + c|(2i)_0 (2i+1)_0\rangle]$, where $|0\rangle, |1\rangle, |2\rangle$ are eigenvectors
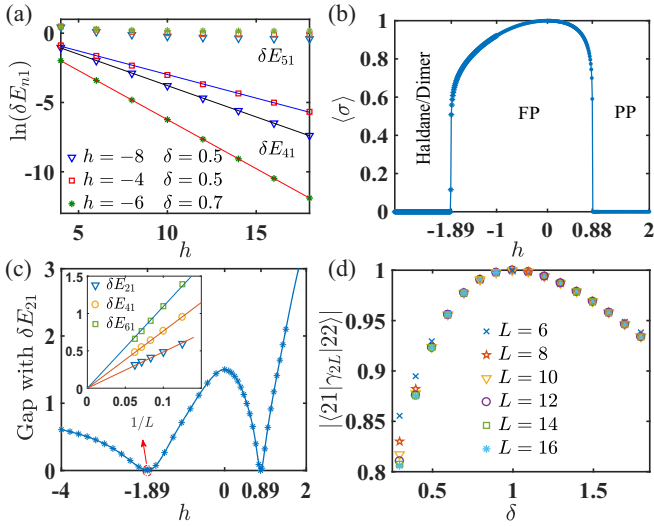
FIG. 3. (a) Level spacing $\delta E_{n1} = E_n - E_1$ with open boundary condition in the emergent Haldane phase. (b) Ferromagnetic order $\Delta = |\langle \sigma \rangle|$ at $\delta = 0.5$ to characterize the boundaries of the FP phase. (c) Energy gap $\delta E_{21}$ in the infinite volume with close boundary condition at $\delta = 0.5$. Inset gives the scaling of $\delta E_{n1}$ at the critical point. (d) Overlap between edge modes and $\gamma_{2L}$ with different chain lengths for $h = -8$.

of $\tau$ with $\tau|i\rangle = \omega^i|i\rangle$ and $c = \frac{1}{2}[\sqrt{36h^2 - 12h + 9} + 6h - 1] \simeq 1/(3|h|) \ll 1$. Thus the ground state is always unique. This regime is termed as dimer phase [16,40,41] and is topologically trivial.

## III. EMERGENT HALDANE PHASE AND TOPOLOGICAL TRANSITION

Here we mainly focus on the properties of the emergent Haldane phase. From the simple picture at $\delta = 1$, $h < 0$, we see that the ground states are fourfold degenerate. We consider a more general case in Fig. 3(a) for a finite system with open boundary conditions based on the ED method. The splitting between the fourth level and the ground state, $\delta E_{41} = E_4 - E_1$, decreases exponentially to zero with increasing length $L$, indicating the exact fourfold degeneracy in infinite volume. This phase is protected by a finite energy gap between the fifth and ground-state levels, i.e., $\lim_{L \to \infty} \delta E_{51}(L)$ is finite. With close boundary conditions [49–51], the edge modes are paired, leading to a unique ground state. In this case we perform the same analysis in Fig. 3(b) and show that the gap $\delta E_{21} = E_2 - E_1$ vanishes only at the phase boundaries. We show in the inset that at the phase boundary, $\delta E_{n1} \propto 1/L$ for all $n > 1$ due to criticality.

We determine the phase boundaries of the FP phase using the ferromagnetic order $\Delta = |\langle \sigma \rangle|$, which is realized in numerical simulation without $\mathbb{Z}_3$ symmetry restriction by writing the Hamiltonian in the eigenvectors of $\sigma$ [42]. This method enables us to precisely determine the phase boundaries due to the sharp transitions from finite value in the FP phase to zero in all other phases, including the Haldane and dimer phases, see Fig. 3(c). Notice that the case for $\delta$ and $-\delta$ give the same

value for $\Delta$, since these two cases can be made to the same upon one lattice translation.

We now discuss the particular properties of the edge modes, which show some distinct features as compared with those from the $\mathbb{Z}_2$ spin models. Let us again consider $\delta = +1$ and $h < 0$. In this case the two left parafermions, $\alpha_1$, $\alpha_2$, and two right parafermions, $\alpha_{2L-1}$, $\alpha_{2L}$, are decoupled from the bulk $H(\alpha_3, \alpha_4, \ldots, \alpha_{2L-3}, \alpha_{2L-2})$. Taking the two left parafermions as an example, we may represent $\alpha_1 = \sigma$ and $\alpha_2 = \omega \sigma \tau$, and then the Hamiltonian can be written as $H = -h(\tau + \tau^\dagger) = -h \, \text{diag}(2, -1, -1)$. We can define the left projector $P_l = |1\rangle\langle 1| + |2\rangle\langle 2| = \text{diag}(0, 1, 1)$, which projects the wave function to the two lowest eigenvectors of $H$, and then we can approximate the two edge modes as $\alpha_i \to \gamma_i = P_l \alpha_i P_l$. We find that $\gamma_1 = \gamma_2$, which are zero modes of the original Hamiltonian, i.e., $[\gamma_1, H] = 0$. Similar results can be found for the right zero modes for $\gamma_{2L} = P_r \alpha_{2L} P_r$. These two modes satisfy the fermionic relation at the same site, $\gamma_1^2 = \gamma_{2L}^2 = 0$, and the parafermionic commute relation between the two ends, $\gamma_1 \gamma_{2L} = \omega \gamma_{2L} \gamma_1$, which mark the important difference between our model and the previous fermionic edge modes [52]. If we denote this state as $|11\rangle$, then the other three zero modes are $|12\rangle = \omega \gamma_{2L}^\dagger |11\rangle$, $|21\rangle = \gamma_1^\dagger |11\rangle$, $|22\rangle = \omega^2 \gamma_{2L}^\dagger |21\rangle$.

The zero modes are exact only in the limiting case of $\delta = 1$, $h < 0$. However, we expect these localized edge modes to be extended to a distance of the order of one correlation length near the open ends [51]. In this case, the exact edge operators at the two ends have a finite overlap with $\gamma_1$ and $\gamma_{2L}$. To this end we diagonalize the Hamiltonian with open boundary conditions at $h = -8$, and calculate the matrix element of $\gamma_{2L}$ between $|22\rangle$ and $|21\rangle$. This overlap depends only on the correlation length when $L$ is large enough. For the result in Fig. 3(d), the correlation length $\xi \sim 1$ when $\delta \to 1$; thus the overlap is saturated even in a short chain.

## IV. LONG-RANGE STRING ORDER

We define the string order as

$$O_s = \lim_{|i-j| \to \infty} \langle \sigma_{2i} U_{2i+1} U_{2i+2} \cdots U_{2j-2} \sigma_{2j-1}^\dagger \rangle, \quad (4)$$

which is generalized from the string order in previous Haldane phases [53–57]. The operator $U_i$ in Eq. (4) is the generator of the charge conjugate symmetry satisfying $U_i \tau_i U_i^\dagger = \tau_i^\dagger$ and $U_i \sigma_i U_i^\dagger = \sigma_i^\dagger$. This string order is not unique; nevertheless, the one in Eq. (4) is enough to distinguish the topological states from the trivial phases. One should notice that when transformed to the parafermion picture, the above string order can be written as $O_s = \lim_{|i-j| \to \infty} \langle \psi_{2i}(U_{2i+1}\tau_{2i+1}) \cdots (U_{2j-2}\tau_{2j-2}) \chi_{2j-1}^\dagger \rangle$ ($\chi_k$, $\psi_k$ are parafermions $\alpha_{2k-1}$, $\alpha_{2k}$ and $\tau_k$ transforms as $\chi_k^\dagger \psi_k$), which is also a nonlocal string. Thus even in the parafermion representation, it possesses all the necessary properties of the symmetry-protected Haldane phase. In Fig. 4, we compute the string order using the infinite-chain DMRG method [58], sweeping along both horizontal and vertical directions on the phase diagram. We find that this string order in the topological phases is nonzero and drops to zero in all trivial phases. From Figs. 4(a) and 4(b), we see that when sweeping from
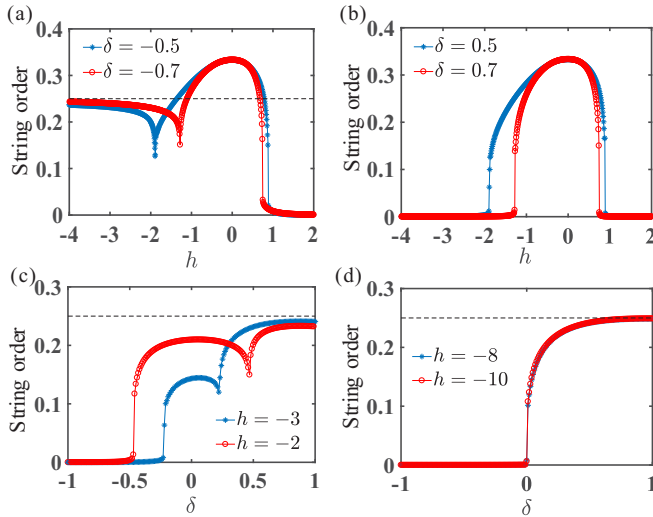
FIG. 4. Long-range string order as a function of $\delta$ (a), (b) and $h$ (c), (d). Results are obtained using infinite-chain DMRG method with bond dimension $m = 200$. The horizontal dashed lines mark the limit of the $\mathbb{Z}_2$ spin model with $O_s = O_s^{xx} = \frac{1}{4}$.

the Haldane phase to the FP and PP phases, the string order undergoes a sudden drop at the phase boundary between the FP and Haldane phases, which was originally determined by ferromagnetic order $\Delta$. In the PP phase, it drops to zero. This is different from the case with $\delta < 0$, in which the string order is zero in both the dimer and PP phases. In Figs. 4(c) and 4(d), we plot the string order as a function of $\delta$, which also exhibits similar features. When $h \ll -4.6$, the string order is reduced to $O_s^{xx} = -\lim_{|i-j| \to \infty} \langle s_{2i}^x s_{2i+1}^x \cdots s_{2j-2}^x s_{2j-1}^\dagger \rangle = 1/4$ [17].

## V. CENTRAL CHARGE AND ENTANGLEMENT SPECTRA

We further characterize the boundaries using entanglement entropy (EE), which in a finite chain with periodic boundary conditions can be written as [44,46,47,59,60]

$$S(x) \sim \frac{c}{3} \ln \left( \frac{L}{\pi} \sin \frac{\pi x}{L} \right), \tag{5}$$

where $x$ is the position of the site and $c$ is the central charge. For the phase boundaries of the FP phase, we find that $c = \frac{4}{5}$. At the phase boundary between the Haldane phase and dimer phase, $c = 1$. One should notice that due to the alternating-bond strengths in our model, the EE also exhibits oscillating behaviors; thus $S(x)$ should be fitted for the odd and even sites, respectively [see Figs. 5(a) and 5(b)].

We provide more insight into the physics in these topological phases from the entanglement spectra $\xi_i = -\ln(\rho_i)$ [51,61–67]. Here, $\rho_i = \hat{\rho}_A = \mathrm{Tr}_B |\psi\rangle\langle\psi|$, where $|\psi\rangle$ is the ground-state wave function, and $A$, $B$ are two partitions of the parafermion chain. As was unveiled in Ref. [51], the spectra $\xi_i$ is threefold degenerate in the FP phase. However, in the Haldane phase, it is characterized by fourfold degeneracy [65]. Our results are presented in Fig. 5(c), in which we used a closed parafermion chain [50,51] with chain length $L = 80$ cut from the center for two partitions. We find that for the lowest eight eigenvalues, they are strictly fourfold degenerate in the Haldane phase. Nevertheless, for the higher spectra,
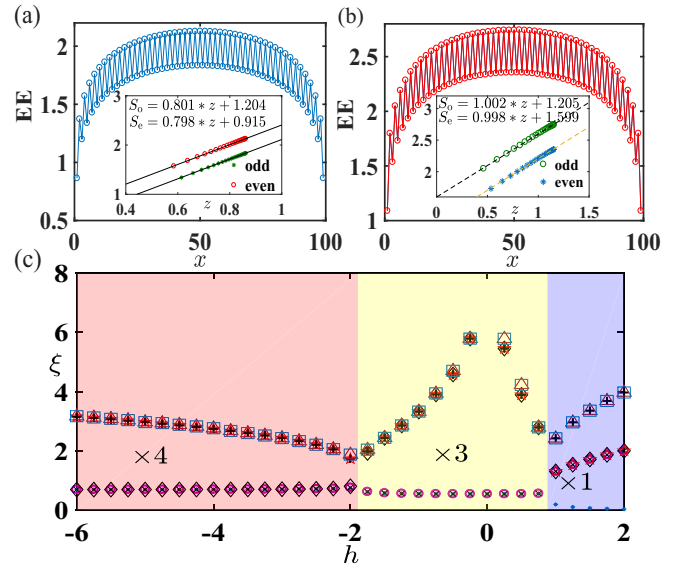


FIG. 5. Von Neumann EE in the phase boundary of FP phase with $h = -1.89$, $\delta = 0.5$ (a) and C phase with $h = -0.22$, $\delta = 1.1$ (b). Results are obtained using periodic boundary condition with bond dimension $m = 2000$. Inset shows the corresponding fitted central charge for the even sites and odd sites, respectively. In the horizontal axis, we set $z = \frac{1}{3}\ln[\frac{L}{\pi} \sin(\pi \frac{x}{L})]$. (c) The lowest eight levels of entanglement spectra in the Haldane phase, FP phase, and PP phase. Results are obtained for $L = 80$, $\delta = 0.5$, bond dimension $m = 2000$ with periodic boundary condition. The ground-state degeneracy for the spectra is marked by $\times 4$, $\times 3$, and $\times 1$ for these three different phases.

their values are vanishingly small but no longer fourfold degenerate. The whole spectra are exactly fourfold degenerate in the limit when the Zeeman field is negative enough. In the FP phase, all the spectra are threefold degenerate, in agreement with the previous observation [51]. In the trivial PP phase, all spectra are not degenerate anymore.

*Topological protection.* We find that the Haldane phase is protected by both charge conjugate symmetry $C = \prod_i U_i \mathcal{K}$ ($\mathcal{K}$ is the complex conjugate operator) with $C^2 = +1$, and $\mathbb{Z}_3$ parity $P = \prod_i \tau_i$ with $P^3 = 1$. The fourfold degeneracy breaks down only for terms violating these two symmetries. Let us define two left(right) edge states, where $P|1\rangle = \omega|1\rangle$ and $P|2\rangle = \omega^2|2\rangle$. By projecting to these two edge modes, we find the projective representation:

$$\mathcal{P}_L = P_l P P_l = \begin{pmatrix} \omega & 0 \\ 0 & \omega^2 \end{pmatrix}, \quad \mathcal{C}_L = P_l C P_l = \begin{pmatrix} 0 & 1 \\ 1 & 0 \end{pmatrix} \mathcal{K}, \tag{6}$$

which satisfy $[H, \mathcal{P}_L \mathcal{C}_L] = 0$ in the ground-state subspace. We find that for any eigenvector $|\psi\rangle$ in the subspace, $\mathcal{P}_L \mathcal{C}_L |\psi\rangle$ is impossible to be identical to $|\psi\rangle$, since $(\mathcal{P}_L \mathcal{C}_L)^2 = \mathcal{P}_L^* \neq 1$. For this reason in each open end the ground states should be twofold degenerate, giving rise to the four edge modes $|ij\rangle$, with parity $\omega^{i+j}$. This idea also applies well to other parafermion models.

To conclude, we investigate the emergent Haldane phase in the $\mathbb{Z}_3$ alternating-bond parafermion chain, which exhibits

fourfold degeneracy in both ground states and entanglement spectra, and is characterized by nonzero long-range string order, generalized from the $\mathbb{Z}_2$ spin models. We find that the FP phase is also characterized by nonzero string order and threefold degeneracy in both ground states and entanglement spectra. The boundaries of the FP phase are critical with $c = \frac{4}{5}$. With our construction, the Haldane phase can also be realized with other $\mathbb{Z}_k$ parafermions. We expect these results to open a new avenue in the search for these exotic topological phases with parafermions.

[1] X.-G. Wen, *Quantum Field Theory of Many-Body Systems* (Oxford University Press, New York, 2004).

[2] X.-G. Wen, Colloquium: Zoo of quantum-topological phases of matter, Rev. Mod. Phys. **89**, 041004 (2017).

[3] E. Witten, Fermion path integrals and topological phases, Rev. Mod. Phys. **88**, 035001 (2016).

[4] C. L. Kane and E. J. Mele, Z2 Topological Order and The Quantum Spin Hall Effect, Phys. Rev. Lett. **95**, 146802 (2005).

[5] F. D. M. Haldane, Continuum dynamics of the 1-D Heisenberg antiferromagnet: Identification with the O(3) nonlinear sigma model, Phys. Lett. A **93**, 464 (1983).

[6] F. D. M. Haldane, Nonlinear Field Theory of Large-Spin Heisenberg Antiferromagnets: Semiclassically Quantized Solitons of the One-Dimensional Easy-Axis Néel State, Phys. Rev. Lett. **50**, 1153 (1983).

[7] M. Z. Hasan and C. L. Kane, Colloquium: Topological insulators, Rev. Mod. Phys. **82**, 3045 (2010).

[8] X.-L. Qi and S.-C. Zhang, Topological insulators and superconductors, Rev. Mod. Phys. **83**, 1057 (2011).

[9] A. Yu. Kitaev, Unpaired Majorana fermions in quantum wires, Phys. Usp. **44**, 131 (2001).

[10] J. Alicea, Y. Oreg, G. Refael, F. Von Oppen, and M. P. A. Fisher, Non-Abelian statistics and topological quantum information processing in 1D wire networks, Nat. Phys. **7**, 412 (2011).

[11] V. Mourik, K. Zuo, S. M. Frolov, S. R. Plissard, E. P. A. M. Bakkers, and L. P. Kouwenhoven, Signatures of Majorana fermions in hybrid superconductor-semiconductor nanowire devices, Science **336**, 1003 (2012).

[12] A. Das, Y. Ronen, Y. Most, Y. Oreg, M. Heiblum, and H. Shtrikman, Zero-bias peaks and splitting in an Al-InAs nanowire topological superconductor as a signature of Majorana fermions, Nat. Phys. **8**, 887 (2012).

[13] M. T. Deng, C. L. Yu, G. Y. Huang, M. Larsson, P. Caroff, and H. Q. Xu, Anomalous zero-bias conductance peak in a Nb-InSb nanowire-Nb hybrid device, Nano Lett. **12**, 6414 (2012).

[14] Q. L. He, L. Pan, A. L. Stern, E. C. Burks, X. Che, G. Yin, J. Wang, B. Lian, Q. Zhou, E. S. Choi *et al.*, Chiral Majorana fermion modes in a quantum anomalous Hall insulator-superconductor structure, Science **357**, 294 (2017).

[15] H. Zhang, C.-X. Liu, S. Gazibegovic, D. Xu, J. A. Logan, G. Wang, N. van Loo, J. D. S. Bommer, M. W. A. de Moor, D. Car, R. L. M. O. het Veld, P. J. van Veldhoven, S. Koelling, M. A. Verheijen, M. Pendharkar, D. J. Pennachio, B. Shojaei, J. S. Lee, C. J. Palmstrøm, E. P. A. M. Bakkers, S. D. Sarma, and L. P. Kouwenhoven, Quantized Majorana conductance, Nature (London) **556**, 74 (2018).

[16] K. Hida, Crossover between the Haldane-gap phase and the dimer phase in the spin-1/2 alternating Heisenberg chain, Phys. Rev. B **45**, 2207 (1992).

[17] K. Hida, Ground-state phase diagram of the spin-1/2 alternating Heisenberg chain, Phys. Rev. B **46**, 8268 (1992).

[18] E. G. Dalla Torre, E. Berg, and E. Altman, Hidden Order in 1D Bose Insulators, Phys. Rev. Lett. **97**, 260401 (2006).

[19] E. Berg, E. G. Dalla Torre, T. Giamarchi, and E. Altman, Rise and fall of hidden string order of lattice bosons, Phys. Rev. B **77**, 245119 (2008).

[20] D. Rossini and R. Fazio, Phase diagram of the extended Bose-Hubbard model, New J. Phys. **14**, 065012 (2012).

[21] G. G. Batrouni, R. T. Scalettar, V. G. Rousseau, and B. Grémaud, Competing Supersolid and Haldane Insulator Phases in the Extended One-Dimensional Bosonic Hubbard Model, Phys. Rev. Lett. **110**, 265303 (2013).

[22] S. Ejima, F. Lange, and H. Fehske, Spectral and Entanglement Properties of the Bosonic Haldane Insulator, Phys. Rev. Lett. **113**, 020401 (2014).

[23] F. Lange, S. Ejima, and H. Fehske, Anyonic Haldane Insulator in One Dimension, Phys. Rev. Lett. **118**, 120401 (2017).

[24] M. Nakagawa and N. Kawakami, Symmetry-protected topological phase transition in one-dimensional Kondo lattice and its realization with ultracold atoms, Phys. Rev. B **96**, 155133 (2017).

[25] L. Barbiero, S. Fazzini, and A. Montorsi, Non-local order parameters as a probe for phase transitions in the extended Fermi-Hubbard model, Eur. Phys. J.: Spec. Top. **226**, 2697 (2017).

[26] L. Barbiero, A. Montorsi, and M. Roncaglia, How hidden orders generate gaps in one-dimensional fermionic systems, Phys. Rev. B **88**, 035109 (2013).

[27] V. Bois, S. Capponi, P. Lecheminant, M. Moliner, and K. Totsuka, Phase diagrams of one-dimensional half-filled two-orbital Su(*N*) cold fermion systems, Phys. Rev. B **91**, 075121 (2015).

[28] P. Fendley, Parafermionic edge zero modes in $\mathbb{Z}_n$-invariant spin chains, J. Stat. Mech.: Theory Exp. (2012) P11020.

[29] A. S. Jermyn, R. S. K. Mong, J. Alicea, and P. Fendley, Stability of zero modes in parafermion chains, Phys. Rev. B **90**, 165106 (2014).

[30] Y. Zhuang, H. J. Changlani, N. M. Tubman, and T. L. Hughes, Phase diagram of the $\mathbb{Z}_3$ parafermionic chain with chiral interactions, Phys. Rev. B **92**, 035154 (2015).

[31] E. M. Stoudenmire, D. J. Clarke, R. S. K. Mong, and J. Alicea, Assembling Fibonacci anyons from a $\mathbb{Z}_3$ parafermion lattice model, Phys. Rev. B **91**, 235112 (2015).

[32] M. Barkeshli and X.-L. Qi, Synthetic Topological Qubits in Conventional Bilayer Quantum Hall Systems, Phys. Rev. X **4**, 041035 (2014).

[33] R. S. K. Mong, D. J. Clarke, J. Alicea, N. H. Lindner, P. Fendley, C. Nayak, Y. Oreg, A. Stern, E. Berg, K. Shtengel *et al.*, Universal Topological Quantum Computation from A Superconductor-Abelian Quantum Hall Heterostructure, Phys. Rev. X **4**, 011036 (2014).

[34] A. Vaezi and M. Barkeshli, Fibonacci Anyons from Abelian Bilayer Quantum Hall States, Phys. Rev. Lett. **113**, 236804 (2014).

[35] J. Alicea and P. Fendley, Topological phases with parafermions: Theory and blueprints, Annu. Rev. Condens. Matter Phys. **7**, 119 (2016).

[36] A. Vaezi, Superconducting Analog of the Parafermion Fractional Quantum Hall States, Phys. Rev. X **4**, 031009 (2014).

[37] D. J. Clarke, J. Alicea, and K. Shtengel, Exotic non-Abelian anyons from conventional fractional quantum Hall states, Nat. Commun. **4**, 1348 (2013).

[38] A. Milsted, E. Cobanera, M. Burrello, and G. Ortiz, Commensurate and incommensurate states of topological quantum matter, Phys. Rev. B **90**, 195101 (2014).

[39] Y. Alavirad, D. Clarke, A. Nag, and J. D. Sau, $\mathbb{Z}_3$ Parafermionic Zero Modes without Andreev Backscattering from the $\frac{2}{3}$ Fractional Quantum Hall State, Phys. Rev. Lett. **119**, 217701 (2017).

[40] Y.-C. Tzeng, L. Dai, M.-C. Chung, L. Amico, and L.-C. Kwek, Entanglement convertibility by sweeping through the quantum phases of the alternating bonds XXZ chain, Sci. Rep. **6**, 26453 (2016).

[41] H. T. Wang, B. Li, and S. Y. Cho, Topological quantum phase transition in bond-alternating spin-1/2 Heisenberg chains, Phys. Rev. B **87**, 054402 (2013).

[42] S.-Y. Zhang, H.-Z. Xu, Y.-X. Huang, G.-C. Guo, Z.-W. Zhou, and M. Gong, Topological phase, supercritical point, and emergent phenomena in an extended parafermion chain, Phys. Rev. B **100**, 125101 (2019).

[43] ITensor library, version 1.2.0, http://itensor.org/.

[44] W. Li, S. Yang, H.-H. Tu, and M. Cheng, Criticality in translation-invariant parafermion chains, Phys. Rev. B **91**, 115133 (2015).

[45] I. Peschel, On the entanglement entropy for an XY spin chain, J. Stat. Mech.: Theory Exp. (2004) P12005.

[46] P. Ginsparg, Applied conformal field theory, arXiv:hep-th/9108028.

[47] P. Calabrese and J. Cardy, Entanglement entropy and quantum field theory, J. Stat. Mech.: Theory Exp. (2004) P06002.

[48] F. Pollmann, S. Mukerjee, A. M. Turner, and J. E. Moore, Theory of Finite-Entanglement Scaling at One-Dimensional Quantum Critical Points, Phys. Rev. Lett. **102**, 255701 (2009).

[49] R. Bondesan and T. Quella, Topological and symmetry broken phases of $\mathbb{Z}_n$ parafermions in one dimension, J. Stat. Mech.: Theory Exp (2013) P10024.

[50] A. Alexandradinata, N. Regnault, C. Fang, M. J. Gilbert, and B. A. Bernevig, Parafermionic phases with symmetry breaking and topological order, Phys. Rev. B **94**, 125103 (2016).

[51] J. Motruk, E. Berg, A. M. Turner, and F. Pollmann, Topological phases in gapped edges of fractionalized systems, Phys. Rev. B **88**, 085115 (2013).

[52] W. P Su, J. R. Schrieffer, and A. J. Heeger, Solitons in Polyacetylene, Phys. Rev. Lett. **42**, 1698 (1979).

[53] M. den Nijs and K. Rommelse, Preroughening transitions in crystal surfaces and valence-bond phases in quantum spin chains, Phys. Rev. B **40**, 4709 (1989).

[54] T. Kennedy and H. Tasaki, Hidden $\mathbb{Z}_2 \times \mathbb{Z}_2$ symmetry breaking in Haldane-gap antiferromagnets, Phys. Rev. B **45**, 304 (1992).

[55] T. Kennedy and H. Tasaki, Hidden symmetry breaking and the Haldane phase in $s = 1$ quantum spin chains, Commun. Math. Phys. **147**, 431 (1992).

[56] D. Pérez-García, M. M. Wolf, M. Sanz, F. Verstraete, and J. I. Cirac, String Order and Symmetries in Quantum Spin Lattices, Phys. Rev. Lett. **100**, 167202 (2008).

[57] F. Pollmann and A. M. Turner, Detection of symmetry-protected topological phases in one dimension, Phys. Rev. B **86**, 125441 (2012).

[58] I. P. McCulloch, Infinite size density matrix renormalization group, revisited, arXiv:0804.2509.

[59] P. Calabrese and J. Cardy, Entanglement entropy and conformal field theory, J. Phys. A: Math. Theor. **42**, 504005 (2009).

[60] G. Vidal, J. I. Latorre, E. Rico, and A. Kitaev, Entanglement in Quantum Critical Phenomena, Phys. Rev. Lett. **90**, 227902 (2003).

[61] H. Li and F. D. M. Haldane, Entanglement Spectrum As a Generalization of Entanglement Entropy: Identification of Topological Order in Non-Abelian Fractional Quantum Hall Effect States, Phys. Rev. Lett. **101**, 010504 (2008).

[62] F. Pollmann, A. M. Turner, E. Berg, and M. Oshikawa, Entanglement spectrum of a topological phase in one dimension, Phys. Rev. B **81**, 064439 (2010).

[63] L. Fidkowski, Entanglement Spectrum of Topological Insulators and Superconductors, Phys. Rev. Lett. **104**, 130502 (2010).

[64] L. Fidkowski and A. Kitaev, Topological phases of fermions in one dimension, Phys. Rev. B **83**, 075103 (2011).

[65] A. M. Turner, F. Pollmann, and E. Berg, Topological phases of one-dimensional fermions: An entanglement point of view, Phys. Rev. B **83**, 075102 (2011).

[66] T. H. Hsieh and L. Fu, Bulk Entanglement Spectrum Reveals Quantum Criticality within a Topological State, Phys. Rev. Lett. **113**, 106801 (2014).

[67] Z.-Q. Wang, G.-Y. Zhu, and G.-M. Zhang, Decoding quantum criticalities from fermionic/parafermionic topological states, Phys. Rev. B **98**, 155139 (2018).